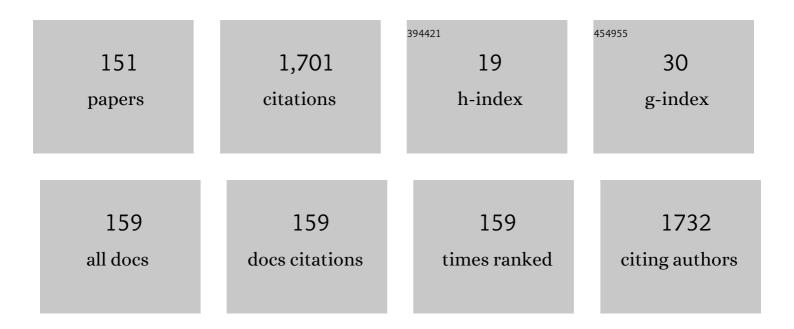
Seigo Kinuya

List of Publications by Year in descending order

Source: https://exaly.com/author-pdf/4547828/publications.pdf Version: 2024-02-01



SEICO KINUVA

| # | Article | IF | CITATIONS |
|----|---|-----|-----------|
| 1 | Prognostic factors for refractory pheochromocytoma and paraganglioma after 1311-metaiodobenzylguanidine therapy. Annals of Nuclear Medicine, 2022, 36, 61-69. | 2.2 | 3 |
| 2 | Phase I/II clinical trial of high-dose [131I] meta-iodobenzylguanidine therapy for high-risk neuroblastoma preceding single myeloablative chemotherapy and haematopoietic stem cell transplantation. European Journal of Nuclear Medicine and Molecular Imaging, 2022, 49, 1574-1583. | 6.4 | 3 |
| 3 | Application of a tungsten apron for occupational radiation exposure in nursing care of children with neuroblastoma during 1311-meta-iodo-benzyl-guanidine therapy. Scientific Reports, 2022, 12, 47. | 3.3 | 2 |
| 4 | Development of Radiohalogenated Osimertinib Derivatives as Imaging Probes for Companion Diagnostics of Osimertinib. Journal of Medicinal Chemistry, 2022, 65, 1835-1847. | 6.4 | 12 |
| 5 | An open-label, single-arm, multi-center, phase II clinical trial of single-dose [1311]meta-iodobenzylguanidine therapy for patients with refractory pheochromocytoma and paraganglioma. Annals of Nuclear Medicine, 2022, 36, 267-278. | 2.2 | 5 |
| 6 | Volumetric evaluation of 99mTc-pyrophosphate SPECT/CT for transthyretin cardiac amyloidosis: Methodology and correlation with cardiac functional parameters. Journal of Nuclear Cardiology, 2022, 29, 3102-3110. | 2.1 | 6 |
| 7 | Safety and response after peptide receptor radionuclide therapy with ¹⁷⁷ Luâ€DOTATATE for neuroendocrine tumors in phase 1/2 prospective Japanese trial. Journal of Hepato-Biliary-Pancreatic Sciences, 2022, 29, 487-499. | 2.6 | 7 |
| 8 | Evaluation of skeletal muscle activity during foot training exercises using positron emission tomography. Scientific Reports, 2022, 12, 7076. | 3.3 | 1 |
| 9 | l-131 metaiodobenzylguanidine therapy is a significant treatment option for pheochromocytoma and paraganglioma. Nuklearmedizin - NuclearMedicine, 2022, 61, 231-239. | 0.7 | 1 |
| 10 | Prediction of multivessel coronary artery disease and candidates for stress-only imaging using multivariable models with myocardial perfusion imaging. Annals of Nuclear Medicine, 2022, 36, 674-683. | 2.2 | 2 |
| 11 | Development of tumor-targeting aza-vesamicol derivatives with high affinity for sigma receptors for cancer theranostics. RSC Medicinal Chemistry, 2022, 13, 986-997. | 3.9 | 1 |
| 12 | The utility of heart-to-mediastinum ratio using a planar image created from IQ-SPECT with Iodine-123 meta-iodobenzylguanidine. Journal of Nuclear Cardiology, 2021, 28, 2569-2577. | 2.1 | 11 |
| 13 | Metal artifact reduction for improving quantitative SPECT/CT imaging. Annals of Nuclear Medicine, 2021, 35, 291-298. | 2.2 | 8 |
| 14 | Real-world safety and effectiveness of radium-223 in Japanese patients with castration-resistant prostate cancer (CRPC) and bone metastasis: exploratory analysis, based on the results of post-marketing surveillance, according to prior chemotherapy status and in patients without concomitant use of second-generation androgen-receptor axis-targeted agents. International Journal | 2.2 | 9 |
| 15 | of Clinical Oncology, 2021, 26, 753-763. A Radiobrominated Tyrosine Kinase Inhibitor for EGFR with L858R/T790M Mutations in Lung Carcinoma. Pharmaceuticals, 2021, 14, 256. | 3.8 | 6 |
| 16 | Skeletal muscle metabolism on whole-body positron emission tomography during pitching. Journal of the International Society of Sports Nutrition, 2021, 18, 21. | 3.9 | 1 |
| 17 | Comparison of the detecting capability between 123I-mIBG and post-therapeutic 131I-mIBG scintigraphy for curie scoring in patients with neuroblastoma after chemotherapy. Annals of Nuclear Medicine, 2021, 35, 649-661. | 2.2 | 1 |
| 18 | Visualization of Dynamic Expression of Myocardial Sigma-1 Receptor After Myocardial Ischemia and Reperfusion Using Radioiodine-Labeled 2-[4-(2-iodophenyl)piperidino]cyclopentanol (OI5V) Imaging. Circulation Journal, 2021, 85, 2102-2108. | 1.6 | 4 |

| # | Article | IF | CITATIONS |
|----|--|-----|-----------|
| 19 | ⁶⁸ Ga- and ²¹¹ At-Labeled RGD Peptides for Radiotheranostics with Multiradionuclides. Molecular Pharmaceutics, 2021, 18, 3553-3562. | 4.6 | 14 |
| 20 | Colchicine treatment early after infarction attenuates myocardial inflammatory response demonstrated by 14C-methionine imaging and subsequent ventricular remodeling by quantitative gated SPECT. Annals of Nuclear Medicine, 2021, 35, 253-259. | 2.2 | 5 |
| 21 | Development of Radiogallium-Labeled Peptides for Platelet-Derived Growth Factor Receptor β (PDGFRβ) Imaging: Influence of Different Linkers. Molecules, 2021, 26, 41. | 3.8 | 14 |
| 22 | Convolutional neural network-based automatic heart segmentation and quantitation in 1231-metaiodobenzylguanidine SPECT imaging. EJNMMI Research, 2021, 11, 105. | 2.5 | 4 |
| 23 | Synthesis and Evaluation of a Dimeric RGD Peptide as a Preliminary Study for Radiotheranostics with Radiohalogens. Molecules, 2021, 26, 6107. | 3.8 | 6 |
| 24 | Feasibility of 125I-RGD uptake as a marker of angiogenesis after myocardial infarction. Annals of Nuclear Medicine, 2021, , 1. | 2.2 | 0 |
| 25 | Synthesis and evaluation of radiogallium-labeled long-chain fatty acid derivatives as myocardial metabolic imaging agents. PLoS ONE, 2021, 16, e0261226. | 2.5 | 1 |
| 26 | Reliability of the muscle strength measurement and effects of the strengthening by an innovative exercise device for the abdominal trunk muscles. Journal of Back and Musculoskeletal Rehabilitation, 2020, 33, 677-684. | 1.1 | 9 |
| 27 | Decreasing undesirable absorbed radiation to the intestine after administration of radium-223 dichloride for treatment of bone metastases. Scientific Reports, 2020, 10, 11917. | 3.3 | 2 |
| 28 | High-dose 1311-mIBG as consolidation therapy in pediatric patients with relapsed neuroblastoma and ganglioneuroblastoma: the Japanese experience. Annals of Nuclear Medicine, 2020, 34, 840-846. | 2.2 | 5 |
| 29 | Diagnostic Use of Post-therapy 131I-Meta-Iodobenzylguanidine Scintigraphy in Consolidation Therapy for Children with High-Risk Neuroblastoma. Diagnostics, 2020, 10, 663. | 2.6 | 7 |
| 30 | Thallium-201 Imaging in Intact Olfactory Sensory Neurons with Reduced Pre-Synaptic Inhibition In Vivo. Molecular Neurobiology, 2020, 57, 4989-4999. | 4.0 | 1 |
| 31 | (â^')―o â€[11 C]methyl―trans â€decalinvesamicol ((â^')â€[11 C]OMDV) as a PET ligand for the vesicular acetylcholine transporter. Synapse, 2020, 74, e22176. | 1.2 | 1 |
| 32 | High-dose 1311-metaiodobenzylguanidine therapy in patients with high-risk neuroblastoma in Japan. Annals of Nuclear Medicine, 2020, 34, 397-406. | 2.2 | 10 |
| 33 | Synthesis and Fundamental Evaluation of Radioiodinated Rociletinib (CO-1686) as a Probe to Lung Cancer with L858R/T790M Mutations of Epidermal Growth Factor Receptor (EGFR). Molecules, 2020, 25, 2914. | 3.8 | 13 |
| 34 | Serial examination of cardiac function and perfusion in growing rats using SPECT/CT for small animals. Scientific Reports, 2020, 10, 160. | 3.3 | 1 |
| 35 | Radiation exposure in nurses during care of 131I-MIBC therapy for pediatric patients with high-risk neuroblastoma. Annals of Nuclear Medicine, 2020, 34, 441-447. | 2.2 | 1 |
| 36 | Calibrated scintigraphic imaging procedures improve quantitative assessment of the cardiac sympathetic nerve activity. Scientific Reports, 2020, 10, 21834. | 3.3 | 7 |

| # | Article | IF | CITATIONS |
|----|---|-----|-----------|
| 37 | Safety and effectiveness of radium-223 dichloride (Ra-223) in patients with mCRPC in real-world setting: A Japanese post-marketing study (PMS) Journal of Clinical Oncology, 2020, 38, 236-236. | 1.6 | 2 |
| 38 | Nasal thalliumâ€201 uptake in patients with parosmia with and without hyposmia after upper respiratory tract infection. International Forum of Allergy and Rhinology, 2019, 9, 1252-1256. | 2.8 | 11 |
| 39 | Fully automated analysis for bone scintigraphy with artificial neural network: usefulness of bone scan index (BSI) in breast cancer. Annals of Nuclear Medicine, 2019, 33, 755-765. | 2.2 | 12 |
| 40 | Postconditioning Accelerates Myocardial Inflammatory Resolution Demonstrated by ¹⁴ C-Methionine Imaging and Attenuates Ventricular Remodeling After Ischemia and Reperfusion. Circulation Journal, 2019, 83, 2520-2526. | 1.6 | 3 |
| 41 | Utility of bone SPECT/CT to identify the primary cause of pain in elderly patients with degenerative lumbar spine disease. Journal of Orthopaedic Surgery and Research, 2019, 14, 185. | 2.3 | 16 |
| 42 | Nuclear medicine practice in Japan: a report of the eighth nationwide survey in 2017. Annals of Nuclear Medicine, 2019, 33, 725-732. | 2.2 | 33 |
| 43 | A phase I clinical trial for [131I]meta-iodobenzylguanidine therapy in patients with refractory pheochromocytoma and paraganglioma. Scientific Reports, 2019, 9, 7625. | 3.3 | 16 |
| 44 | Ability of artificial intelligence to diagnose coronary artery stenosis using hybrid images of coronary computed tomography angiography and myocardial perfusion SPECT. European Journal of Hybrid Imaging, 2019, 3, 4. | 1.5 | 10 |
| 45 | Radiotheranostics Coupled between an At-211-Labeled RGD Peptide and the Corresponding Radioiodine-Labeled RGD Peptide. ACS Omega, 2019, 4, 4584-4591. | 3.5 | 31 |
| 46 | ☆Symposium: Imaging modalities for drug-related osteonecrosis of the jaw (5), utility of bone scintigraphy and 18F-FDG PET/CT in early detection and risk assessment of medication-related osteonecrosis of the jaw (secondary publication). Japanese Dental Science Review, 2019, 55, 76-79. | 5.1 | 8 |
| 47 | Syntheses and evaluation of a homologous series of aza-vesamicol as improved radioiodine-labeled probes for sigma-1 receptor imaging. Bioorganic and Medicinal Chemistry, 2019, 27, 1990-1996. | 3.0 | 5 |
| 48 | An appreciation from the out-going editor-in-chief. Annals of Nuclear Medicine, 2019, 33, 875-876. | 2.2 | 0 |
| 49 | Impact of iterative reconstruction with resolution recovery in myocardial perfusion SPECT: phantom and clinical studies. Scientific Reports, 2019, 9, 19618. | 3.3 | 4 |
| 50 | Prognostic Value of Early Evaluation of Left Ventricular Dyssynchrony After Myocardial Infarction. Molecular Imaging and Biology, 2019, 21, 654-659. | 2.6 | 5 |
| 51 | Activities for the Development of Targeted Radionuclide Therapy in Japan. Nuclear Medicine and Molecular Imaging, 2019, 53, 35-37. | 1.0 | 2 |
| 52 | Design, synthesis, and biological evaluation of radioiodinated benzo[d]imidazole-quinoline derivatives for platelet-derived growth factor receptor β (PDGFRβ) imaging. Bioorganic and Medicinal Chemistry, 2019, 27, 383-393. | 3.0 | 7 |
| 53 | Fundamental study of radiogallium-labeled aspartic acid peptides introducing octreotate derivatives. Annals of Nuclear Medicine, 2019, 33, 244-251. | 2.2 | 6 |
| 54 | Accuracy of an artificial neural network for detecting a regional abnormality in myocardial perfusion SPECT. Annals of Nuclear Medicine, 2019, 33, 86-92. | 2.2 | 16 |

| # | Article | IF | CITATIONS |
|----|---|-----|-----------|
| 55 | Introduction of the targeted alpha therapy (with Radium-223) into clinical practice in Japan: learnings and implementation. Annals of Nuclear Medicine, 2019, 33, 211-221. | 2.2 | 16 |
| 56 | Utility of I-MIBG Standardized Uptake Value in Patients with Refractory Pheochromocytoma and Paraganglioma. Asia Oceania Journal of Nuclear Medicine and Biology, 2019, 7, 115-120. | 0.1 | 0 |
| 57 | Artificial neural network retrained to detect myocardial ischemia using a Japanese multicenter database. Annals of Nuclear Medicine, 2018, 32, 303-310. | 2.2 | 24 |
| 58 | ls 123I-metaiodobenzylguanidine heart-to-mediastinum ratio dependent on age? From Japanese Society of Nuclear Medicine normal database. Annals of Nuclear Medicine, 2018, 32, 175-181. | 2.2 | 17 |
| 59 | Manual on the proper use of lutetium-177-labeled somatostatin analogue (Lu-177-DOTA-TATE) injectable in radionuclide therapy (2nd ed.). Annals of Nuclear Medicine, 2018, 32, 217-235. | 2.2 | 41 |
| 60 | Quantification of Myocardial Perfusion Defect Size in Rats: Comparison between Quantitative Perfusion SPECT and Autoradiography. Molecular Imaging and Biology, 2018, 20, 544-550. | 2.6 | 4 |
| 61 | Current Consensus on I-131 MIBG Therapy. Nuclear Medicine and Molecular Imaging, 2018, 52, 254-265. | 1.0 | 57 |
| 62 | Objective evaluation of cerebrovascular reactivity for acetazolamide predicts cerebral hyperperfusion after carotid artery stenting: Comparison with region of interest methods. Journal of Neuroradiology, 2018, 45, 362-367. | 1.1 | 6 |
| 63 | Creation and characterization of normal myocardial perfusion imaging databases using the IQ·SPECT system. Journal of Nuclear Cardiology, 2018, 25, 1328-1337. | 2.1 | 17 |
| 64 | Comparison of Radioiodine- or Radiobromine-Labeled RGD Peptides between Direct and Indirect Labeling Methods. Chemical and Pharmaceutical Bulletin, 2018, 66, 651-659. | 1.3 | 23 |
| 65 | Imaging Somatostatin Receptor Activity in Neuroendocrine-differentiated Prostate Cancer. Internal Medicine, 2018, 57, 3123-3128. | 0.7 | 9 |
| 66 | Feasibility of High-dose Iodine-131-metaiodobenzylguanidine Therapy for High-risk Neuroblastoma Preceding Myeloablative Chemotherapy and Hematopoietic Stem Cell Transplantation: a Study Protocol. Asia Oceania Journal of Nuclear Medicine and Biology, 2018, 6, 161-166. | 0.1 | 2 |
| 67 | Comparison of phase dyssynchrony analysis using gated myocardial perfusion imaging with four software programs: Based on the Japanese Society of Nuclear Medicine working group normal database. Journal of Nuclear Cardiology, 2017, 24, 611-621. | 2.1 | 63 |
| 68 | IQ-SPECT for thallium-201 myocardial perfusion imaging: effect of normal databases on quantification. Annals of Nuclear Medicine, 2017, 31, 454-461. | 2.2 | 5 |
| 69 | Characteristics of single- and dual-photopeak energy window acquisitions with thallium-201 IQ-SPECT/CT system. Annals of Nuclear Medicine, 2017, 31, 529-535. | 2.2 | 6 |
| 70 | Comparison of diagnostic performance of four software packages for phase dyssynchrony analysis in gated myocardial perfusion SPECT. EJNMMI Research, 2017, 7, 27. | 2.5 | 30 |
| 71 | Prognostic value of olfactory nerve damage measured with thallium-based olfactory imaging in patients with idiopathic olfactory dysfunction. Scientific Reports, 2017, 7, 3581. | 3.3 | 12 |
| 72 | Bone scan index of the jaw: a new approach for evaluating early-stage anti-resorptive agents-related osteonecrosis. Annals of Nuclear Medicine, 2017, 31, 201-210. | 2.2 | 19 |

| # | Article | IF | CITATIONS |
|----|--|-----|-----------|
| 73 | Validation of Left Ventricular Ejection Fraction with the IQ•SPECT System in Small-Heart Patients. Journal of Nuclear Medicine Technology, 2017, 45, 201-207. | 0.8 | 8 |
| 74 | Influence of Attenuation Correction by Brain Perfusion SPECT/CT Using a Simulated Abnormal Bone Structure: Comparison Between Chang and CT Methods. Journal of Nuclear Medicine Technology, 2017, 45, 208-213. | 0.8 | 2 |
| 75 | Reducing the small-heart effect in pediatric gated myocardial perfusion single-photon emission computed tomography. Journal of Nuclear Cardiology, 2017, 24, 1378-1388. | 2.1 | 14 |
| 76 | Complete remission of metastatic pheochromocytoma in 123I-metaiodobenzylguanidine scintigraphy after a single session of 131I-metaiodobenzylguanidine therapy: a case report. BMC Research Notes, 2017, 10, 750. | 1.4 | 0 |
| 77 | A phase I clinical trial for [¹³¹ I]meta-iodobenzylguanidine therapy in patients with refractory pheochromocytoma and paraganglioma: a study protocol. Journal of Medical Investigation, 2017, 64, 205-209. | 0.5 | 7 |
| 78 | Innovative exercise device for the abdominal trunk muscles: An early validation study. PLoS ONE, 2017, 12, e0172934. | 2.5 | 16 |
| 79 | Molecular Imaging for Personalized Medicine. BioMed Research International, 2016, 2016, 1-1. | 1.9 | 2 |
| 80 | In Vivo Differences between Two Optical Isomers of Radioiodinated o-iodo-trans-decalinvesamicol for Use as a Radioligand for the Vesicular Acetylcholine Transporter. PLoS ONE, 2016, 11, e0146719. | 2.5 | 2 |
| 81 | Cardiac Time-of-flight PET for Evaluating Myocardial Perfusion with ¹³ N-ammonia. Annals of Nuclear Cardiology, 2016, 2, 73-78. | 0.2 | 2 |
| 82 | Evaluation of cytological radiation damage to lymphocytes after I-131 metaiodobenzylguanidine therapy by the cytokinesis-blocked micronucleus assay. Annals of Nuclear Medicine, 2016, 30, 624-628. | 2.2 | 2 |
| 83 | Optimization of the filter parameters in 99mTc myocardial perfusion SPECT studies: the formulationÂof flowchart. Australasian Physical and Engineering Sciences in Medicine, 2016, 39, 571-581. | 1.3 | 3 |
| 84 | Development of a myocardial phantom and analysis system toward the standardization of myocardial SPECT image across institutions. Annals of Nuclear Medicine, 2016, 30, 699-707. | 2.2 | 4 |
| 85 | New section in EJNMMI and Annals of Nuclear Medicine. Annals of Nuclear Medicine, 2016, 30, 593-593. | 2.2 | 4 |
| 86 | Synthesis and evaluation of a new vesamicol analog o-[11C]methyl-trans-decalinvesamicol as a PET ligand for the vesicular acetylcholine transporter. Annals of Nuclear Medicine, 2016, 30, 122-129. | 2.2 | 8 |
| 87 | 30th anniversary of Annals of Nuclear Medicine. Annals of Nuclear Medicine, 2016, 30, 1-2. | 2.2 | 2 |
| 88 | Simultaneous acquisition of 99mTc- and 123I-labeled radiotracers using a preclinical SPECT scanner with CZT detectors. Annals of Nuclear Medicine, 2016, 30, 263-271. | 2.2 | 11 |
| 89 | Triple-phase contrast-enhanced MRI for the prediction of preoperative chemotherapeutic effect in patients with osteosarcoma: comparison with 99mTc-MIBI scintigraphy. Skeletal Radiology, 2016, 45, 87-95. | 2.0 | 11 |
| 90 | Effects of the belt electrode skeletal muscle electrical stimulation system on lower extremity skeletal muscle activity: Evaluation using positron emission tomography. Journal of Orthopaedic Science, 2016, 21, 53-56. | 1.1 | 31 |

| # | Article | IF | CITATIONS |
|-----|---|-----|-----------|
| 91 | Development and validation of a direct-comparison method for cardiac 123I-metaiodobenzylguanidine washout rates derived from late 3-hour and 4-hour imaging. European Journal of Nuclear Medicine and Molecular Imaging, 2016, 43, 319-325. | 6.4 | 14 |
| 92 | Cardiac Time-of-flight PET for Evaluating Myocardial Perfusion with ¹³ N-ammonia. Annals of Nuclear Cardiology, 2016, 2, 73-78. | 0.2 | 1 |
| 93 | Correlation between apoptosis and left ventricular remodeling in subacute phase of myocardial ischemia and reperfusion. EJNMMI Research, 2015, 5, 72. | 2.5 | 13 |
| 94 | Iodine-131 Metaiodobenzylguanidine Therapy for Neuroblastoma: Reports So Far and Future Perspective. Scientific World Journal, The, 2015, 2015, 1-9. | 2.1 | 33 |
| 95 | Reproducibility Between Brain Uptake Ratio Using Anatomic Standardization and Patlak-Plot Methods. Journal of Nuclear Medicine Technology, 2015, 43, 261-266. | 0.8 | 0 |
| 96 | In vivo radioactive metabolite analysis for individualized medicine: A basic study of a new method of CYP activity assay using 1231-IMP. Nuclear Medicine and Biology, 2015, 42, 171-176. | 0.6 | 1 |
| 97 | Effect of postconditioning on dynamic expression of tenascin-C and left ventricular remodeling after myocardial ischemia and reperfusion. EJNMMI Research, 2015, 5, 21. | 2.5 | 9 |
| 98 | Draft guidelines regarding appropriate use of 1311-MIBG radiotherapy for neuroendocrine tumors. Annals of Nuclear Medicine, 2015, 29, 543-552. | 2.2 | 19 |
| 99 | Extremity Radioactive Iodine Uptake on Post-therapeutic Whole Body Scan in Patients with Differentiated Thyroid Cancer. Asia Oceania Journal of Nuclear Medicine and Biology, 2015, 3, 26-34. | 0.1 | 3 |
| 100 | Nuclear medicine practice in Japan: a report of the seventh nationwide survey in 2012. Annals of Nuclear Medicine, 2014, 28, 1032-1038. | 2.2 | 22 |
| 101 | Diagnostic utility of 123I-BMIPP imaging in patients with Takotsubo cardiomyopathy. Journal of Cardiology, 2014, 64, 49-56. | 1.9 | 36 |
| 102 | Effects and safety of 1311-metaiodobenzylguanidine (MIBG) radiotherapy in malignant neuroendocrine tumors: Results from a multicenter observational registry. Endocrine Journal, 2014, 61, 1171-1180. | 1.6 | 41 |
| 103 | Current status and perspective of targeted radionuclide therapy for cancer. Drug Delivery System, 2014, 29, 294-303. | 0.0 | 2 |
| 104 | Bone scintigraphy as a new imaging biomarker: the relationship between bone scan index and bone metabolic markers in prostate cancer patients with bone metastases. Annals of Nuclear Medicine, 2013, 27, 802-807. | 2.2 | 45 |
| 105 | A new parameter of bone scintigraphy: Relation between bone scan index and bone metabolic markers in prostate cancer patients with bone metastases Journal of Clinical Oncology, 2013, 31, e16072-e16072. | 1.6 | 0 |
| 106 | Thyroid hormone replacement one day before (131)I therapy in patients with well-differentiated thyroid cancer. Asia Oceania Journal of Nuclear Medicine and Biology, 2013, 1, 20-6. | 0.1 | 1 |
| 107 | Evaluation of Cardiac Mitochondrial Function by a Nuclear Imaging Technique using Technetium-99m-MIBI Uptake Kinetics. Asia Oceania Journal of Nuclear Medicine and Biology, 2013, 1, 39-43. | 0.1 | 3 |
| 108 | I-131-Metaiodobenzylguanidine therapy with allogeneic cord blood stem cell transplantation for recurrent neuroblastoma. Italian Journal of Pediatrics, 2012, 38, 53. | 2.6 | 5 |

| # | Article | IF | CITATIONS |
|-----|---|-----|-----------|
| 109 | A nuclear power plant accident in Fukushima: what should we do?. Annals of Nuclear Medicine, 2012, 26, 113-114. | 2.2 | 4 |
| 110 | Thyroid remnant ablation using 1,110ÂMBq of I-131 after total thyroidectomy: regulatory considerations on release of patients after unsealed radioiodine therapy. Annals of Nuclear Medicine, 2012, 26, 370-378. | 2.2 | 14 |
| 111 | Comparison of Diagnostic Value of I-123 MIBG and High-Dose I-131 MIBG Scintigraphy Including Incremental Value of SPECT/CT Over Planar Image in Patients With Malignant Pheochromocytoma/Paraganglioma and Neuroblastoma. Clinical Nuclear Medicine, 2011, 36, 1-7. | 1.3 | 70 |
| 112 | Biodistribution of humanized anti-VEGF monoclonal antibody/bevacizumab on peritoneal metastatic models with subcutaneous xenograft of gastric cancer in mice. Cancer Chemotherapy and Pharmacology, 2010, 66, 745-753. | 2.3 | 19 |
| 113 | Nuclear medicine practice in Japan: a report of the sixth nationwide survey in 2007. Annals of Nuclear Medicine, 2009, 23, 209-215. | 2.2 | 12 |
| 114 | Preparation and evaluation of 186/188Re-labeled antibody (A7) for radioimmunotherapy with rhenium(I) tricarbonyl core as a chelate site. Annals of Nuclear Medicine, 2009, 23, 843-848. | 2.2 | 13 |
| 115 | Intraperitoneal radioimmunotherapy to treat the early phase of peritoneal dissemination of human colon cancer cells in a murine model. Nuclear Medicine Communications, 2007, 28, 129-133. | 1.1 | 15 |
| 116 | Airway complication occurring during radioiodine treatment for Graves' disease. Annals of Nuclear Medicine, 2007, 21, 367-369. | 2.2 | 12 |
| 117 | 99mTc-sestamibi to monitor treatment with antisense oligodeoxynucleotide complementary to MRP mRNA in human breast cancer cells. Annals of Nuclear Medicine, 2006, 20, 29-34. | 2.2 | 5 |
| 118 | Respiratory distress caused by radioiodine therapy in patients with differentiated thyroid cancer. Annals of Nuclear Medicine, 2006, 20, 499-502. | 2.2 | 5 |
| 119 | Anti-angiogenic therapy and chemotherapy affect 99mTc sestamibi and 99mTc-HL91 accumulation differently in tumour xenografts. Nuclear Medicine Communications, 2005, 26, 1067-1073. | 1.1 | 3 |
| 120 | Locoreginal radioimmunotherapy with Re-labeled monoclonal antibody in treating small peritoneal carcinomatosis of colon cancer in mice in comparison with I-counterpart. Cancer Letters, 2005, 219, 41-48. | 7.2 | 28 |
| 121 | Multifactorial analysis on the short-term side effects occurring within 96 hour after radioiodine-131 therapy for differentiated thyroid carcinoma. Annals of Nuclear Medicine, 2004, 18, 345-349. | 2.2 | 60 |
| 122 | Failure of radioiodine treatment in Graves' disease intentionally caused by a patient: Suspected Munchausen syndrome. Annals of Nuclear Medicine, 2004, 18, 631-632. | 2.2 | 1 |
| 123 | Single dose planning for radioiodine-131 therapy of Graves' disease. Annals of Nuclear Medicine, 2004, 18, 151-155. | 2.2 | 11 |
| 124 | Improved survival of mice bearing liver metastases of colon cancer cells treated with a combination of radioimmunotherapy and antiangiogenic therapy. European Journal of Nuclear Medicine and Molecular Imaging, 2004, 31, 981-5. | 6.4 | 9 |
| 125 | In vitro detection of mdr1 mRNA in murine leukemia cells with 111In-labeled oligonucleotide. European Journal of Nuclear Medicine and Molecular Imaging, 2004, 31, 1523-1529. | 6.4 | 10 |
| 126 | Limitations of 99mTc tetrofosmin in assessing reversal effects of verapamil on the function of multi-drug resistance associated protein 1. Nuclear Medicine Communications, 2004, 25, 585-589. | 1.1 | 0 |

| # | Article | IF | CITATIONS |
|-----|---|-----|-----------|
| 127 | Hypoxia as a factor for 67Ga accumulation in tumour cells. Nuclear Medicine Communications, 2004, 25, 49-53. | 1.1 | 12 |
| 128 | Local delivery of 131 I-MIBG to treat peritoneal neuroblastoma. European Journal of Nuclear Medicine and Molecular Imaging, 2003, 30, 1246-1250. | 6.4 | 4 |
| 129 | Reduction of 99m Tc-sestamibi and 99m Tc-tetrofosmin uptake in MRP-expressing breast cancer cells under hypoxic conditions is independent of MRP function. European Journal of Nuclear Medicine and Molecular Imaging, 2003, 30, 1529-1531. | 6.4 | 15 |
| 130 | Feasibility of 186 Re-radioimmunotherapy for treatment in an adjuvant setting of colon cancer. Journal of Cancer Research and Clinical Oncology, 2003, 129, 392-396. | 2.5 | 14 |
| 131 | Intraperitoneal radioimmunotherapy in treating peritoneal carcinomatosis of colon cancer in mice compared with systemic radioimmunotherapy. Cancer Science, 2003, 94, 650-654. | 3.9 | 19 |
| 132 | Radioimmunotherapy with 186Re-Labeled Monoclonal Antibody to Treat Liver Metastases of Colon Cancer Cells in Nude Mice. Cancer Biotherapy and Radiopharmaceuticals, 2002, 17, 681-687. | 1.0 | 11 |
| 133 | Hypoxia-induced alteration of tracer accumulation in cultured cancer cells and xenografts in mice: implications for pre-therapeutic prediction of treatment outcomes with 99mTc-sestamibi, 201Tl chloride and 99mTc-HL91. European Journal of Nuclear Medicine and Molecular Imaging, 2002, 29, 1006-1011. | 6.4 | 17 |
| 134 | Benefits of combined radioimmunotherapy and anti-angiogenic therapy in a liver metastasis model of human colon cancer cells. European Journal of Nuclear Medicine and Molecular Imaging, 2002, 29, 1669-1674. | 6.4 | 20 |
| 135 | Cooperative effect of radioimmunotherapy and antiangiogenic therapy with thalidomide in human cancer xenografts. Journal of Nuclear Medicine, 2002, 43, 1084-9. | 5.0 | 12 |
| 136 | Improved response of colon cancer xenografts to radioimmunotherapy with pentoxifylline treatment. European Journal of Nuclear Medicine and Molecular Imaging, 2001, 28, 750-755. | 2.1 | 8 |
| 137 | Anti-angiogenic therapy and radioimmunotherapy in colon cancer xenografts. European Journal of Nuclear Medicine and Molecular Imaging, 2001, 28, 1306-1312. | 2.1 | 19 |
| 138 | Experimental radioimmunotherapy with186Re-MAG3-A7 anti-colorectal cancer monoclonal antibody: Comparison with131I-counterpart. Annals of Nuclear Medicine, 2001, 15, 199-202. | 2.2 | 11 |
| 139 | Clinical approach to renal study incidental to99mTc-MDP bone scintigraphy. Annals of Nuclear Medicine, 2001, 15, 237-245. | 2.2 | 3 |
| 140 | Esophageal hypomotility in systemie sclerosis: Close relationship with pulmonary involvement. Annals of Nuclear Medicine, 2001, 15, 97-101. | 2.2 | 28 |
| 141 | Technetium-99m-Tetrofosmin Would Be a Substrate for Multidrug Resistance-associated Protein (MRP): Comparison between a Leukemia Cell Line with High MRP Gene Expression and Its Parental Cell Line. Cancer Biotherapy and Radiopharmaceuticals, 2001, 16, 17-23. | 1.0 | 9 |
| 142 | Enhanced Efficacy of Radioimmunotherapy Combined with Systemic Chemotherapy and Local Hyperthermia in Xenograft Model. Japanese Journal of Cancer Research, 2000, 91, 573-578. | 1.7 | 10 |
| 143 | Increased uptake of99mTc-HL91 in tumor cells exposed to X-ray radiation. Annals of Nuclear Medicine, 2000, 14, 139-141. | 2.2 | 5 |
| 144 | Optimal Timing of Administration of Hyperthermia in Combined Radioimmunotherapy. Cancer Biotherapy and Radiopharmaceuticals, 2000, 15, 373-379. | 1.0 | 7 |

| # | Article | IF | CITATIONS |
|-----|---|-----|-----------|
| 145 | Efficacy, toxicity and mode of interaction of combination radioimmunotherapy with 5-fluorouracil in colon cancer xenografts. Journal of Cancer Research and Clinical Oncology, 1999, 125, 630-636. | 2.5 | 17 |
| 146 | Combination radioimmunotherapy with local hyperthermia: increased delivery of radioimmunoconjugate by vascular effect and its retention by increased antigen expression in colon cancer xenografts. Cancer Letters, 1999, 140, 209-218. | 7.2 | 15 |
| 147 | Rhenium-186-mercaptoacetyltriglycine-labeled Monoclonal Antibody for Radioimmunotherapy:In vitroAssessment,in vivoKinetics and Dosimetry in Tumor-bearing Nude Mice. Japanese Journal of Cancer Research, 1998, 89, 870-880. | 1.7 | 15 |
| 148 | 99mTc-tetrofosmin uptake in bone metastases from breast cancer. Annals of Nuclear Medicine, 1998, 12, 293-296. | 2.2 | 2 |
| 149 | Short-period-induced hypertension could improve tumor-to-nontumor ratios of radiolabeled monoclonal antibody. Nuclear Medicine and Biology, 1997, 24, 547-551. | 0.6 | 7 |
| 150 | Intense Ga-67 uptake in adenosquamous carcinoma of the pancreas. Annals of Nuclear Medicine, 1997, 11, 41-43. | 2.2 | 20 |
| 151 | Effect of induced hypertension with angiotensin II infusion on biodistribution of 111In-labeled monoclonal antibody. Nuclear Medicine and Biology, 1996, 23, 137-140. | 0.6 | 9 |